

MOL #81364

**Mithramycin A inhibits myeloid cell leukemia-1 to induce apoptosis in oral squamous cell carcinomas and tumor xenograft through activation of Bax and oligomerization**

Ji-Ae Shin, Ji-Youn Jung, Mi Heon Ryu, Stephen Safe, Sung-Dae Cho

Department of Oral Pathology, School of Dentistry and Institute of Oral Bioscience, Brain Korea 21 project, Chonbuk National University, Jeon-ju, Republic of Korea (J.-A.S., S.-D.C.)

Department of Companion and Laboratory Animal Science, Kongju National University, Yesan, Republic of Korea (J.-Y.J.)

Department of Oral Pathology, School of Dentistry, Yangsan Campus of Pusan National University, Beomeo-ri, Mulgeum-eup, Yangsan, Republic of Korea (M.H.R)

Department of Veterinary Physiology and Pharmacology, Texas A&M University, 4466 TAMU, Vet. Res. Bldg. 410, College Station, TX 77843-4466, and Institute of Biosciences and Technology, Texas A&M University Health Science Center, 2012W Holcomebe Blvd, Houston, TX 77030-3303, USA (S.S)

MOL #81364

**Running title:** Mithramycin A inhibits Mcl-1 and induces apoptosis

**Correspondence to:**

Sung-Dae Cho assistant professor, DVM PhD

Department of Oral Pathology, School of Dentistry and Institute of Oral Bioscience, Chonbuk

National University, Jeonju, 561-756, Republic of Korea

Tel: 82-63-270-4027; Fax: 82-63-270-4025

E-mail: [efiwdsc@chonbuk.ac.kr](mailto:efiwdsc@chonbuk.ac.kr)

The number of text pages: 29

The number of figures: 5

The number of references: 39

The number of words in the Abstract: 229

The number of words in the Introduction: 457

The number of words in the Discussion: 1020

**Abbreviations:**

Mcl-1, myeloid cell leukemia-1; OSCC, oral squamous cell carcinoma; TPA, 12-O-tetradecanoylphorbol-13-acetate; EGF, epidermal growth factor; RNAi, RNA interference; Mith, mithramycin A; Bcl-2, B-cell lymphoma-2; NSAID, non-steroidal anti-inflammatory drug; NOM, normal oral mucosa; PARP, poly (ADP-ribose) polymerase; Cox4, cytochrome c oxidase polypeptide IV; RT-PCR, reverse transcription-polymerase chain reaction; MTS, 3-(4,5-dimethylthiazol-20yl)-(3-carboxymethoxyphenyl)-2-(4-sulphophenyl)-2H-tetrazolium; DAPI, 4'-6-diamidino-2-phenylindole; BMH, bismaleimide; TUNEL, terminal deoxynucleotidyl transferase dUTP nick-end labeling.

MOL #81364

## Abstract

In several human malignancies, overexpression of myeloid cell leukemia-1 (Mcl-1) confers resistance to induction of apoptosis; however, Mcl-1-mediated inhibition of apoptosis in oral squamous cell carcinoma (OSCC) is not fully understood and has been investigated in this study. The Mcl-1 promoter activators, 12-O-tetradecanoylphorbol-13-acetate (TPA) and epidermal growth factor (EGF) enhanced neoplastic transformation of JB6 cells and this response was accompanied by enhanced expression of Mcl-1, and knockdown of Mcl-1 by RNA interference (RNAi) decreased JB6 cell transformation. In the same cell line, we also demonstrated that mithramycin A (Mith) decrease TPA-induced JB6 cell transformation and Mcl-1 expression. Mcl-1 was over-expressed in human oral tumors compared to normal oral mucosa and also in several OSCC cell lines including HN22 and HSC-4 cells. Treatment of these cells with Mith also decreased Mcl-1 expression and neoplastic cell transformation and this was accompanied by induction of several markers of apoptosis. Knockdown of Mcl-1 by RNAi also induced apoptotic cell death. The downregulation of Mcl-1 by Mith and RNAi increased pro-apoptotic protein Bax, resulting in the Bax translocation into mitochondria and its oligomerization. Mith also suppressed tumor growth *in vivo* and induced apoptosis in tumor by also regulating expression of Mcl-1 and Bax proteins. These indicate a critical role for Mcl-1 in the growth and survival of OSCC and demonstrate that Mith may be a potential anticancer drug candidate for clinical treatment of OSCC.

MOL #81364

## Introduction

Human oral squamous cell carcinoma (OSCC) is the most common neoplasm of oral cavity cancers and the incidence of this carcinoma has been increasing (Liang et al., 2008; Silverman, 2001). Most patients are diagnosed with OSCC only after the disease has reached an advanced stage and the five-year survival rate of oral cancer patients remains relatively low. The optimal treatment or therapy for OSCC remains a controversial and surgery is an effective, but complex method for treatment of OSCC and the development of novel therapeutic regimens to prevent and treat OSCC is critically important.

Myeloid cell leukemia-1 (Mcl-1) is a member of the B-cell lymphoma-2 (Bcl-2) family protein and has been characterized as a critical survival factor for hematopoietic-derived cells such as multiple myeloma cell lines (Opferman et al., 2005). The prosurvival functions of Mcl-1 are due to interacting with proapoptotic members of the Bcl-2 family such as Bim, Bak, and Bax and this results in the inhibition of cytochrome c release from the mitochondria and decreased apoptosis (Kazi et al., 2011; Zhang et al., 2011). Recently, it has been reported that Mcl-1 is overexpressed in tumor cells of human primary OSCC and cultured SCC cell lines suggesting that Mcl-1 may be an important drug target for treatment of human OSCC cases (Nagata et al., 2009). Our group also recently reported that downregulation of Mcl-1 by non-steroidal anti-inflammatory drug (NSAID), tolfenamic acid induced apoptosis in YD-15 mucoepidermoid carcinoma cells, major malignant carcinoma of the salivary gland (Choi et al., 2011b). However, these studies did not identify the molecular mechanisms and linkages between tolfeniamc acid-dependent downregulation of Mcl-1 and induction of apoptosis in YD-15 cells.

Mithramycin A (Mith) is a chemotherapeutic compound which has been used in the therapy of several types of cancer (Koller & Miller., 1986). It also called plicamycin and Mith

MOL #81364

binds to a GC-rich DNA sequences and regulates expression of Sp1, other Sp proteins and Sp-regulated genes including surviving, cyclin D1 and VEGF which also have GC-rich promoter sequences (Abdelrahim et al., 2002; Abdelrahim et al., 2004; Chadalapaka et al., 2008). Most studies with Mith-related studies have been focused on the anti-cancer activity of Mith due to its suppression of Sp1 protein (Jia et al., 2010; Seznec et al., 2011). Recently, we have reported that Mith can modulate expression of both Sp1 and Mcl-1 proteins indicating that this drug may be important for targeting Mcl-1 overexpressing tumors where Mcl-1 play an antiapoptotic function (Choi et al., 2011b). In the present study, we sought to determine the role of Mcl-1 in OSCC and the anti-tumor activity of Mith in OSCC cells in culture and tumors in a xenograft model for oral cancer. We also explored the underlying molecular mechanism associated with Mith-mediated inhibition of Mcl-1.

MOL #81364

## **Materials and Methods**

### **Chemicals and antibodies**

Mithramycin A (Mith) and 12-O-tetradecanoylphorbol-13-acetate (TPA) were supplied by Sigma-Aldrich (Louis, MO, USA). Epidermal growth factor (EGF) was obtained from Invitrogen (Carlsbad, CA, USA). PARP and Bax (6A7) antibodies were purchased from BD Pharmingen™ (San Jose, CA, USA). Sp1 and actin antibodies were obtained from Santa Cruz Biotechnology, Inc. (Santa Cruz, CA, USA). Antibodies against Mcl-1, Bax, cleaved caspase-3 and cleaved caspase-9 were supplied by Cell Signaling Technology, Inc. (Charlottesville, VA, USA). Cox4 antibody was obtained from Abcam (Cambridge, UK).

### **Materials**

Fourteen normal oral mucosa (NOM) tissues and twenty-five oral squamous cell carcinoma (OSCC) tissues were obtained from adult patients who visited the Pusan National University Dental Hospital (Pusan, Korea). Samples were obtained during third molar removal. Twenty-Five cases of OSCC with good preservation of paraffin tissue and hematoxylin/eosin-stained slides were obtained from files of the Department of Pathology, Pusan National University School of Medicine between January 2002 and December 2007. The ethics committee of Pusan National University School of Medicine and Dentistry approved the methods used in the present study.

### **Cell culture and chemical treatment**

HN22 cells were kindly provided by Dankook University (Cheonan, Korea) and HSC4 and HSC2 cells were provided by Hokkaido University (Hokkaido, Japan). Cells were cultured in DMEM supplemented with 10% FBS and antibiotics at 37°C in a 5% CO<sub>2</sub> incubator. Cells

MOL #81364

were treated with DMSO or various concentrations of Mith A (15, 30 or 60 nM) for different time points. JB6 mouse skin epidermal cells were obtained from American Tissue Culture Collection (Manassas, VA, USA), and cells were cultured in MEM supplemented with 5% FBS. JB6 cells were treated with various concentrations of TPA (5, 10 or 20 ng/ml) or EGF (5, 10 or 20 ng/ml) for different time points.

#### **Anchorage-independent cell transformation assay (Soft agar assay)**

JB6 cells were treated with various concentrations (5, 10 or 20 ng/ml) of TPA or EGF in 1ml of 0.3% basal medium Eagle's agar containing 10% FBS. The culture was incubated at 37°C in a 5% CO<sub>2</sub> incubator for 10 days, and then colonies were counted. JB6 treated with 20 ng/ml of TPA, HSC4 and HSC2 cells exposed to various concentrations of Mith A were incubated for 10 days (JB6 cells) or 20 days (HSC4 and HSC2 cells), and then colonies were counted.

#### **Western blot analysis**

Whole cell lysates were extracted with lysis buffer and protein concentrations were measured using a DC Protein Assay (Bio-RAD Laboratories. Hercules, CA, USA). Samples containing equal amounts of protein were separated by SDS-PAGE and then transferred to Immun-Blot™ PVDF membranes (Bio-RAD Laboratories. Hercules, CA, USA). The membranes were blocked with 5% skim milk in TBST at room temperature for 2 hr, and incubated overnight at 4°C with primary antibodies against PARP, cleaved caspase-3, cleaved caspase-9, Sp1, Mcl-1, Bax, Bax (6A7), COX4 or actin, followed by incubation with HRP-conjugated secondary antibodies. Antibody-bound proteins were detected using an ECL Western Blotting Luminol reagent (Santa Cruz, CA, USA).

MOL #81364

### **RNA interference**

On TARGETplus SMARTpool siRNA sequences targeting Mcl-1 and non-targeting control were purchased from Dharmacon Research (Lafayette, CO, USA). Briefly, cells were seeded on 6-well plates, and transiently transfected with 50 nM siRNA for 72 hr using a DhamaFECT2 transfection reagent (Thermo Scientific, Lafayette, CO, USA). After transfection, cells were analyzed by soft agar assay, DAPI staining and Western blot analysis.

### **Immunohistochemistry**

Tissue sections, 4- $\mu$ m thick, were deparaffinized, treated in 100% alcohol, and subjected to avidin-biotin complexation. For antigen retrieval, sections were boiled in pH 6.0 citric buffer using a hot plate for 1 hr, and then cooled for 25 min at room temperature (RT). Endogenous peroxidase was blocked with 3.5% H<sub>2</sub>O<sub>2</sub> solution for 20 min, and then the sections were treated with 15% normal goat serum for 30 min. Primary antibodies were then applied overnight at 4°C, after which secondary antibodies were applied for 20 min. Lastly, sections were visualized with freshly prepared DAB substrate, counterstained with Mayer's hematoxylin, and then mounted and examined under a light microscope. To analyze sections, five non-overlapping fields per slide were randomly selected and images were captured with a light microscope attached to a digital camera (Olympus, BX51T, Tokyo, Japan, X100). The captured images were examined independently in a blinded manner by two experienced oral pathologists. The expression levels of Mcl-1 were categorized into four easily reproducible subgroups as follows: (a) No detectable expression (Point 0); (b) positive expression in less than 30% of cells (Point 1); (c) positive expression in 30-50% of cells (Point 2); (d) positive expression in greater than 50% of cells (Point 3).



MOL #81364

### **Reverse transcription-polymerase chain reaction (RT-PCR)**

Total RNA was extracted from easy-BLUE™ Total RNA Extraction Kit (iNtRON, Daejeon, Korea). cDNA was prepared from 1 µg of total RNA using the ImProm-II™ Reverse Transcription System (Promega, Madison, WI, USA). Mcl-1 and  $\beta$ -Actin transcripts were amplified by PCR using specific primers; Mcl-1 sense 5'-TGC TGG AGT TGG TCG GGG AA-3', Mcl-1 anti-sense 5'-TCG TAA GGT CTC CAG CGC CT-3',  $\beta$ -Actin sense 5'-GTG GGG CGC CCC AGG CAC CA-3',  $\beta$ -Actin anti-sense 5'-CTC CTT AAT GTC ACG CAC GAT TTC-3'. Mcl-1 amplification was done for 28 cycles (1 min at 95°C, 1 min at 60°C, and 1 min 30 sec at 72°C) and  $\beta$ -Actin amplification was done for 25 cycles (1 min at 95°C, 1 min at 60°C, and 1 min 30 sec at 72°C). PCR products were analyzed by 2% agarose gel electrophoresis and visualized by ethidium bromide staining.

### **MTS assay**

The effects of Mithramycin A on cell viability of HN22 and HSC4 cells were determined by the CellTiter 96<sup>R</sup> Aqueous One Solution Cell Proliferation Assay Kit (Promega, Madison, WI, USA) according to the manufacturer's instructions. Briefly, cells were seeded in 96-well plates and then incubated with various concentrations (15, 30, 60 nM) of Mithramycin A for different times (24 or 48 hr). MTS (3-(4,5-dimethylthiazol-20yl)-(3-carboxymethoxyphenyl)-2-(4-sulphophenyl)-2H-tetrazolium) solution was added to each well and maintained for 2 hr at 37°C. The absorbance was measured at 490 nm and 690 nm (background) using an ELISA microplate reader (BIO-TEK Instruments, Inc., Madison, WI, USA).

### **DAPI staining**

MOL #81364

Detection of nuclear fragmentation and chromatin condensation in nuclei of apoptotic cells was carried out using a fluorescent nuclear dye, DAPI (4'-6-diamidino-2-phenylindole, Sigma, Louis, MO, USA). HN22 and HSC4 cells treated with Mithramycin A or transfected with Mcl-1 siRNA were harvested by trypsinization and fixed in 100% methanol at room temperature for 10 min. Cells were deposited on slides, and stained with DAPI solution (2 µg/ml). The cell morphology was observed under a fluorescence microscope.

### **Preparation of cytosolic and mitochondrial fractions**

Cytosolic and mitochondrial fractions were isolated by digitonin or triton X-100 permeabilization. Briefly, cells were washed with ice-cold PBS, and cell pellets were resuspended for 1 min on room temperature in plasma membrane extraction buffer containing 0.05% digitonin. Following a centrifugation step at 15,000 g at 4°C for 5 min, the supernatant was separated from the pellet consisting of cellular debris. The supernatant containing cytosolic proteins was collected, and the mitochondrial pellet was harvested by centrifugation at 15,000 g at 4°C for 5 min. The pellet consisting of mitochondrial proteins was resuspended by plasma membrane extraction buffer containing 0.5% triton X-100. The supernatant containing mitochondrial proteins was collected from last centrifugation.

### **Detection of Bax activation**

HN22 and HSC4 cells treated with Mithramycin A or transfected with Mcl-1 siRNA were harvested and then whole cell lysates were extracted by lysis buffer. The extracted proteins were analyzed by Western blot. Bax activation was detected using primary antibody recognizing only the active form of Bax (6A7).

MOL #81364

### **Cross-linking**

HN22 and HSC4 cells were treated with DMSO or Mithramycin A for 48 hr, and then cells were harvested. For Bax oligomerization, the cells were suspended by conjugation buffer with 10 mM EDTA. The cell lysates were incubated with 0.2 mM Bismaleimide (Thermo scientific, Rockford, IL, USA) at room temperature for 1 hr, and then extracted by lysis buffer for Western blot analysis.

### **Nude mouse xenograft assay**

Female nude mice were purchased from Orient Ltd (Suwon, Korea), and maintained in accordance with the Institutional Animal Care Use Committee guidelines. HN22 cells were implanted with s.c. injection into the flanks of the mice. Mice were divided into two groups of five and the control group received an equal volume of the vehicle, and the treatment group received 0.2 mg/kg/d of Mith five times per week for 46 days. After 46 days, body, organ and tumor weights were measured, and tumor volumes were determined. The tumors were measured along the two diameter axis with calipers to allow a calculation of tumor volume,  $V = \pi / 6 \{ (D + d) / 2 \}^3$ , where D and d are the larger and smaller diameters, respectively.

### **TUNEL assay**

The tumor tissues were analyzed by Dead-End Colorimetric TUNEL System (Promega, Madison, WI, USA) according to the manufacturer's instructions. Briefly, paraffin-embedded slides were deparaffinized and rehydrated. The sections were treated with proteinase K for 15 min at room temperature, and then the endogenous peroxidase was blocked with 0.3% H<sub>2</sub>O<sub>2</sub> in PBS for 5 min. The Digoxigenine-dUTP end labelled DNA was detected using an

MOL #81364

antidigoxigenin-peroxidase antibody, followed by peroxidase detection with 0.05% DAB containing 0.02% H<sub>2</sub>O<sub>2</sub>. The sections were then counterstained with methyl green. The brown colored apoptotic bodies in the tumor sections of the control and Mithramycin A-treated mice were counted using a Nikon Eclipse E800 microscope (Nikon Inc., Melville, NY, USA) at X20 magnification.

### **Statistical analysis**

Data are assessed as means  $\pm$  S.D. of triplicate samples from at least three independent experiments. Statistical significance was evaluated using a Student's t-test or one-way ANOVA and considered significant when  $p < 0.05$ .

MOL #81364

## Results

Normal mouse epidermal JB6 cells readily undergo neo-transformation after treatment with EGF or TPA, Mcl-1 promoter activator. Thus, the JB6 cells treated with EGF or TPA serve as an initial model cells for investigating the relationship between Mcl-1 expression and neoplastic cell transformation. Results in Figure 1A show that in the absence of these mitogens, a minimal number of colonies were observed in an anchorage-independent cell transformation assay. In contrast, treatment with 5-20 ng/ml TPA or EGF significantly increased anchorage-independent growth. Previous studies show that TPA and EGF induce Mcl-1(Booy et al., 2011; Kozopas et al., 1993; Leu et al., 2000) and results in Figure 1B confirm that both mitogens induce a time-dependent increase in Mcl-1 levels which are maximal after 2-6 hr and then decrease at longer time points (9-12 hr); Figure 1C illustrates the dose-dependent induction of Mcl-1 by EGF and TPA at the 3 hr time point. The role of Mcl-1 in TPA and EGF-mediated transformation was determined by RNA interference (RNAi) in the anchorage-independent assay in JB6 cells transfected with control oligonucleotide and a small inhibitory RNA for Mcl-1 (siMcl-1). The results show that knockdown of Mcl-1 significantly inhibited TPA- and EGF-induced JB6 cells transformation (Figure. 1D) and these data demonstrate the critical role of Mcl-1 in mitogen-induced transformation using JB6 cells as a model.

Analysis of normal oral mucosa (NOM) and OSCC tissues (14 and 25 respectively) shows that Mcl-1 expression is significantly higher in tumor vs. non-tumor tissues and high Mcl-1 levels were also observed in several oral cancer cell lines (Figure. 2A). Previous studies showed that Mith, a drug that blocks expression of Sp1 and other Sp transcription factors inhibits Mcl-1 expression in mucoepidermoid carcinoma cells(Choi et al., 2011b) and results in Figure 2B and 2C show that Mith also decreased expression of Mcl-1 protein and

MOL #81364

mRNA levels in HN22 and HSC4 cells. Moreover, Mith also coordinately decreased Mcl-1 and induced PARP cleavage at similar time points in both cell lines after treatment for 24-48 hr whereas minimal effects were observed at earlier time points (Figure. 2D). We also confirmed that Mith inhibited TPA-induced neotransformation of JB6 cells (Figure. 2E) and this correlated with the observed interactions of TPA and Mcl-1 knockdown in these cells (Figures. 1B and 1D). Mith also inhibited anchorage-independent in HSC2 and HSC4 oral cancer cells (Figure. 2F).

Since Mcl-1 is an important survival gene (Akgul, 2009; Mandelin and Pope, 2007; Yang-Yen, 2006), we further investigated the effects of Mith on HN22 and HSC4 cell growth and activation of caspases, which are markers of apoptosis. Figure 3A illustrates that treatment with 15-60 nM Mith significantly inhibited growth of the OSCC cell lines and Mith also induced cleaved caspases-3 and 9 and PARP cleavage in these cell lines after treatment for 48 hr (Figure. 3B). Mith-induced apoptosis in HN22 and HSC4 cells was also confirmed by DAPI staining which showed a dose-dependent increase in apoptotic cells (Figure. 3C). The linkage between Mith-mediated down-regulation of Mcl-1 and induction of apoptosis was confirmed by RNAi using siMcl-1 oligonucleotide. Knockdown of Mcl-1 in HN22 and HSC4 cells induced activation (cleavage) of caspase-3 and caspase-9 and this was accompanied by increased PARP cleavage (Figure. 3D) and increased DAPI staining for apoptotic cells (Figure. 3E). These results demonstrate that the proapoptotic activity of Mith is due to down-regulation of Mcl-1.

Previous studies have demonstrated that the proapoptotic activity of Mcl-1 down-regulation is also linked to induction of Bax (Cheng et al., 2010) and results in Figure 4A show that Mith induces Bax [total protein and activated Bax (6A7)] expression in HN22 and HSC4 cells. Moreover, we also observed that Mith increased mitochondrial levels of Bax

MOL #81364

(Figure. 4B) and Bax oligomerization (Figure. 4C). The role of Mcl-1 knockdown in mediating Bax expression was investigated by RNAi (siMcl-1) and loss of Mcl-1 significantly increased total Bax protein in HSC4, but not in HN22 cells (Figure 4D). However, knockdown of Mcl-1 significantly induced Bax (6A7) proteins in both HN22 and HSC4 cells and this is consistent with a previous reports showing that quercetin downregulates Mcl-1 and induces Bax in U937 cells (Cheng et al., 2010) (Figure. 4E). Moreover, siMcl-1 increased levels of mitochondrial Bax protein whereas it did not decrease total or cytosolic Bax protein expression suggesting that the loss of Mcl-1 in HN22 and HSC4 cells primarily effects the subcellular distribution of Bax which is increased in mitochondria (Figure. 4F).

We also investigated the *in vivo* anti-tumorigenic activity of Mith (0.2 mg/kg/day) in an athymic nude mouse xenograft model using HN22 cells and observed inhibition of tumor volume and weight (Figure. 5A) and this was not accompanied by changes in body weights (Figure. 5B). Analysis of tumor lysates by western blots showed decreased expression of Mcl-1 and no significant changes in Bax protein levels in tumors from animals treated with Mith compared to controls (Figure. 5C). However, Mith clearly increased cleaved caspase 3 and active Bax (6A7) which is consistent with *in vitro* data from HN22 cells (Figures 4D, 4E and 5C). Mith also increased TUNEL-positive cells indicating apoptotic cell death (Figure 5D). We also found that Mith did not affect organ weights or levels of Mcl-1 protein in those organs obtained from Mith- and control-treated mice (Figure 5E). Moreover, histopathological findings showed that there were no differences of organs between from the control- and Mith-treated group indicating no systemic toxicity at the dose of Mith used in this study (Figure 5F).

MOL #81364

## Discussion

Numerous human cancers are typically resistant to apoptosis and aberrant expression of the prosurvival Mcl-1 protein has been identified in many tumors (Erovic et al., 2005; Fleischer et al., 2006; Krajewska et al., 1996; Song et al., 2005). Immortalization of hematopoietic cells and high incidence of lymphomas in transgenic mice over-expressing Mcl-1 supports a role for this protein in tumorigenesis and cancer cell survival (Craig, 2002; Zhou et al., 2001; Zhou et al., 1998). Down-regulation of Mcl-1 also enhances the sensitivity to diverse apoptotic stimuli in various cancer cells (Rahmani et al., 2005; Song et al., 2005; Taniai et al., 2004). In the present study, we showed that Mcl-1 protein is highly expressed in OSCC tissues compared to normal oral mucosa and inhibition of Mcl-1 induced caspase-dependent apoptosis. We also found that Mcl-1 was induced along with neoplastic cell transformation in JB6 cells treated with TPA or EGF and knockdown of Mcl-1 by RNAi inhibited JB6 cell transformation (Figure 1). The linkage between Mcl-1 and cell transformation was also observed in HN22 and HSC4 OSCC cells; knockdown of Mcl-1 by RNAi decreased cell transformation and they were accompanied by induction of apoptosis.

Mith is an aureolic acid-type polyketide identified from a variety of strains of the bacterium *Streptomyces* and has been used to treat Paget's disease (Koller and Miller, 1986). Mith suppresses the expression of the human melanoma-associated gene ABCB8 and has potential therapeutic applications for treating melanoma patients (Sachrajda and Ratajewski, 2011). Mith also decreased VEGF and XIAP to induce apoptosis and inhibit tumor cell migration in glioma cells (Seznec et al., 2011). Analogues of Mith also possess anticancer properties and this is due, in part, to modulate the activity of Sp transcription factors as a new strategy for treatment of metastatic prostate cancer (Malek et al., 2012). In addition, treatment with a combination of Mith and other compounds downregulates Sp1 protein expression and



MOL #81364

exhibits synergistic antitumor activity in pancreatic cancer (Gao et al., 2011). We also investigated the anti-proliferative effects of Mith on OSCC and showed that Mith decreased all growth; in addition Mith also decreased expression of Mcl-1 protein in a concentration- and time-dependent manner and this was accompanied by inhibition of neoplastic cell transformation and induction of apoptosis. These results suggested that Mith may also be a potential drug for targeting Mcl-1 and treatment of OSCC. We also investigated the effects of Mith on other Bcl-2 family members to rule out the involvement of other Bcl-2 family members. The results showed that only Bcl-xL was affected by Mith in both cell lines indicating that Mith-mediated downregulation of Bcl-xL may also play a role in the induction of apoptosis (supplement Figure). Future studies will investigate the molecular pathways related to a role for Bcl-xL in Mith-induced apoptosis in oral cancer. Previously, we reported that tolfenamic acid decreased Mcl-1 mRNA, promoter activity and protein levels showing effects on transcription (Choi et al., 2011a) whereas downregulation of Mcl-1 by sorafenib was due to inhibition of translation (Rahmani et al., 2005). In this study we show that Mith clearly decreased levels of Mcl-1 mRNA and protein (Figures 2B and 2C) indicating that Mith also acts as the transcriptional level.

Previous studies show that Mcl-1 interacts with Bak in adenovirus-infected cells and HeLA cells (Cuconati et al., 2003; Willis et al., 2005). Mcl-1 decreases Bak expression and inhibits its function by inhibiting conformational changes in several cancer cells. Thus, we hypothesized that knockdown of Mcl-1 may also increase Bak protein levels in OSCC and the results showed that down-regulation of Mcl-1 by Mith either did not affect or slightly decreased Bak protein expression (data not shown). Although inhibition of Bak by Mcl-1 has been suggested to play a critical role in its anti-apoptotic characteristic, the relationship between Mcl-1 and Bax is less well understood. Higher expression of Mcl-1 has previously

MOL #81364

been known to inhibit Bax activation (Antonsson et al., 2001). Bax is a cytosolic monomer and activation induces conformational changes (becoming 6A7-positive) and translocation into the outer mitochondria membrane (Antonsson et al., 2001; Leber et al., 2007). Recently, it was reported that the pro-survival activity of Mcl-1 is due to inhibition of Bax function at mitochondria and the anticancer drug, quercetin blocks this response in leukemia cells (Cheng et al., 2010; Germain et al., 2008). Our results also showed that knock-down of Mcl-1 by RNAi or treatment with Mith activated Bax protein (6A7) and induced Bax translocation into mitochondria (Figure 4). We also observed that siMcl-1 and Mith induced Bax oligomerization which proceeds the release of cytochrome c from the outer mitochondria membrane.

Previous reports show that Mith suppresses pancreatic tumor growth in a xenograft model (Yuan et al., 2007). And we also observed that Mith inhibited tumor volume and weight in mice bearing HN22 cells as a xenograft (Figures 5A and 5B). Mith also decreased Mcl-1 expression, activated caspase3 and increased TUNEL-positive cells and activated Bax protein in tumors (Figures 5C and 5D). These results were consistent with *in vitro* data. A previous study reported 0.4 and 1.5 mg/kg doses of Mith had significant systemic side effects as evidenced by a loss of body weight whereas 0.05 mg/kg dose did not cause their side effects (Jia et al., 2010). Another report showed that 0.25 mg/kg Mith did not show toxicity in a pancreatic tumor model (Yuan et al., 2007) and based on these results, we selected a 0.2mg/kg dose for this study and observed no detectable cytotoxic effects based on histopathology and changes in body and organ weights. We also observed that Mith did not alter Mcl-1 protein expression in five organs/tissues obtained from Mith-treated mice compared to controls.

MOL #81364

In summary, our results show that Mcl-1 is overexpressed in oral tumors and cancer cells and results of RNAi experiments and treatment with Mith demonstrate that Mcl-1 exhibits pro-oncogenic activity in oral cancer cells and tumors. Mcl-1 plays a critical role in suppressing activation of Bax and Bax-induced apoptotic responses and Mith effectively downregulates Mcl-1 resulting in inhibition of oral cancer cells and tumor growth. These results suggest that Mith may have important clinical potential as an anticancer drug for treating OSCC.

### **Authorship Contributions**

Participated in research design: Sung-Dae Cho

Conducted experiments: Ji-Ae Shin, Ji-Youn Jung, and Mi Heon Ryu

Performed data analysis: Stephen Safe and Sung-Dae Cho

Wrote or contributed to the writing of the manuscript: Stephen Safe and Sung-Dae Cho

MOL #81364

## References

- Abdelrahim M, Samudio I, Smith R, 3rd, Burghardt R, and Safe S (2002) Small inhibitory RNA duplexes for Sp1 mRNA block basal and estrogen-induced gene expression and cell cycle progression in MCF-7 breast cancer cells. *J Biol Chem* **277**:28815-28822.
- Abdelrahim M, Smith R, 3rd, Burghardt R, and Safe S (2004) Role of Sp proteins in regulation of vascular endothelial growth factor expression and proliferation of pancreatic cancer cells. *Cancer Res* **64**:6740-6749.
- Akgul C (2009) Mcl-1 is a potential therapeutic target in multiple types of cancer. *Cell Mol Life Sci* **66**:1326-1336.
- Antonsson B, Montessuit S, Sanchez B, and Martinou JC (2001) Bax is present as a high molecular weight oligomer/complex in the mitochondrial membrane of apoptotic cells. *J Biol Chem* **276**:11615-11623.
- Booy EP, Henson ES, and Gibson SB (2011) Epidermal growth factor regulates Mcl-1 expression through the MAPK-Elk-1 signalling pathway contributing to cell survival in breast cancer. *Oncogene* **30**:2367-2378.
- Chadalapaka G, Jutooru I, Chintharlapalli S, Papineni S, Smith R, 3rd, Li X, and Safe S (2008) Curcumin decreases specificity protein expression in bladder cancer cells. *Cancer Res* **68**:5345-5354.

MOL #81364

Cheng S, Gao N, Zhang Z, Chen G, Budhraj A, Ke Z, Son YO, Wang X, Luo J, and Shi X (2010) Quercetin induces tumor-selective apoptosis through downregulation of Mcl-1 and activation of Bax. *Clin Cancer Res* **16**:5679-5691.

Choi ES, Shim JH, Jung JY, Kim HJ, Choi KH, Shin JA, Nam JS, Cho NP, and Cho SD (2011a) Apoptotic effect of tolfenamic acid in androgen receptor-independent prostate cancer cell and xenograft tumor through specificity protein 1. *Cancer Sci* **102**:742-748.

Choi KH, Shim JH, Huong LD, Cho NP, and Cho SD (2011b) Inhibition of myeloid cell leukemia-1 by tolfenamic acid induces apoptosis in mucoepidermoid carcinoma. *Oral Dis* **17**:469-475.

Craig RW (2002) MCL1 provides a window on the role of the BCL2 family in cell proliferation, differentiation and tumorigenesis. *Leukemia* **16**:444-454.

Cuconati A, Mukherjee C, Perez D, and White E (2003) DNA damage response and MCL-1 destruction initiate apoptosis in adenovirus-infected cells. *Genes Dev* **17**:2922-2932.

Erovc BM, Pelzmann M, Grasl M, Pammer J, Kornek G, Brannath W, Selzer E, and Thurnher D (2005) Mcl-1, vascular endothelial growth factor-R2, and 14-3-3sigma expression might predict primary response against radiotherapy and chemotherapy in patients with locally advanced squamous cell carcinomas of the head and neck. *Clin Cancer Res* **11**:8632-8636.

MOL #81364

Fleischer B, Schulze-Bergkamen H, Schuchmann M, Weber A, Biesterfeld S, Muller M, Krammer PH, and Galle PR (2006) Mcl-1 is an anti-apoptotic factor for human hepatocellular carcinoma. *Int J Oncol* **28**:25-32.

Gao Y, Jia Z, Kong X, Li Q, Chang DZ, Wei D, Le X, Suyun H, Huang S, Wang L, and Xie K (2011) Combining betulinic acid and mithramycin a effectively suppresses pancreatic cancer by inhibiting proliferation, invasion, and angiogenesis. *Cancer Res* **71**:5182-5193.

Germain M, Milburn J, and Duronio V (2008) MCL-1 inhibits BAX in the absence of MCL-1/BAX Interaction. *J Biol Chem* **283**:6384-6392.

Jia Z, Gao Y, Wang L, Li Q, Zhang J, Le X, Wei D, Yao JC, Chang DZ, Huang S, and Xie K (2010) Combined treatment of pancreatic cancer with mithramycin A and tolfenamic acid promotes Sp1 degradation and synergistic antitumor activity. *Cancer Res* **70**:1111-1119.

Kazi A, Sun J, Doi K, Sung SS, Takahashi Y, Yin H, Rodriguez JM, Becerril J, Berndt N, Hamilton AD, Wang HG, and Sebt SM (2011) The BH3 alpha-helical mimic BH3-M6 disrupts Bcl-X(L), Bcl-2, and MCL-1 protein-protein interactions with Bax, Bak, Bad, or Bim and induces apoptosis in a Bax- and Bim-dependent manner. *J Biol Chem* **286**:9382-9392.

Koller CA, and Miller DM (1986) Preliminary observations on the therapy of the myeloid blast phase of chronic granulocytic leukemia with plicamycin and hydroxyurea. *N Engl J Med* **315**:1433-1438.

MOL #81364

Kozopas KM, Yang T, Buchan HL, Zhou P, and Craig RW (1993) MCL1, a gene expressed in programmed myeloid cell differentiation, has sequence similarity to BCL2. *Proc Natl Acad Sci U S A* **90**:3516-3520.

Krajewska M, Krajewski S, Epstein JI, Shabaik A, Sauvageot J, Song K, Kitada S, and Reed JC (1996) Immunohistochemical analysis of bcl-2, bax, bcl-X, and mcl-1 expression in prostate cancers. *Am J Pathol* **148**:1567-1576.

Leber B, Lin J, and Andrews DW (2007) Embedded together: the life and death consequences of interaction of the Bcl-2 family with membranes. *Apoptosis* **12**:897-911.

Leu CM, Chang C, and Hu C (2000) Epidermal growth factor (EGF) suppresses staurosporine-induced apoptosis by inducing mcl-1 via the mitogen-activated protein kinase pathway. *Oncogene* **19**:1665-1675.

Liang XH, Lewis J, Foote R, Smith D, and Kademani D (2008) Prevalence and significance of human papillomavirus in oral tongue cancer: the Mayo Clinic experience. *J Oral Maxillofac Surg* **66**:1875-1880.

Malek A, Nunez LE, Magistri M, Brambilla L, Jovic S, Carbone GM, Moris F, and Catapano CV (2012) Modulation of the activity of sp transcription factors by mithramycin analogues as a new strategy for treatment of metastatic prostate cancer. *PLoS One* **7**:e35130.

MOL #81364

Mandelin AM, 2nd, and Pope RM (2007) Myeloid cell leukemia-1 as a therapeutic target.

*Expert Opin Ther Targets* **11**:363-373.

Nagata M, Wada K, Nakajima A, Nakajima N, Kusayama M, Masuda T, Iida S, Okura M,

Kogo M, and Kamisaki Y (2009) Role of myeloid cell leukemia-1 in cell growth of squamous cell carcinoma. *J Pharmacol Sci* **110**:344-353.

Opferman JT, Iwasaki H, Ong CC, Suh H, Mizuno S, Akashi K, and Korsmeyer SJ (2005)

Obligate role of anti-apoptotic MCL-1 in the survival of hematopoietic stem cells. *Science* **307**:1101-1104.

Rahmani M, Davis EM, Bauer C, Dent P, and Grant S (2005) Apoptosis induced by the

kinase inhibitor BAY 43-9006 in human leukemia cells involves down-regulation of Mcl-1 through inhibition of translation. *J Biol Chem* **280**:35217-35227.

Sachrajda I, and Ratajewski M (2011) Mithramycin A suppresses expression of the human

melanoma-associated gene ABCB8. *Mol Genet Genomics* **285**:57-65.

Seznec J, Silkenstedt B, and Naumann U (2011) Therapeutic effects of the Sp1 inhibitor

mithramycin A in glioblastoma. *J Neurooncol* **101**:365-377.

Silverman S, Jr. (2001) Demographics and occurrence of oral and pharyngeal cancers. The

outcomes, the trends, the challenge. *J Am Dent Assoc* **132 Suppl**:7S-11S.



MOL #81364

Song L, Coppola D, Livingston S, Cress D, and Haura EB (2005) Mcl-1 regulates survival and sensitivity to diverse apoptotic stimuli in human non-small cell lung cancer cells. *Cancer Biol Ther* **4**:267-276.

Taniai M, Grambihler A, Higuchi H, Werneburg N, Bronk SF, Farrugia DJ, Kaufmann SH, and Gores GJ (2004) Mcl-1 mediates tumor necrosis factor-related apoptosis-inducing ligand resistance in human cholangiocarcinoma cells. *Cancer Res* **64**:3517-3524.

Willis SN, Chen L, Dewson G, Wei A, Naik E, Fletcher JI, Adams JM, and Huang DC (2005) Proapoptotic Bak is sequestered by Mcl-1 and Bcl-xL, but not Bcl-2, until displaced by BH3-only proteins. *Genes Dev* **19**:1294-1305.

Yang-Yen HF (2006) Mcl-1: a highly regulated cell death and survival controller. *J Biomed Sci* **13**:201-204.

Yuan P, Wang L, Wei D, Zhang J, Jia Z, Li Q, Le X, Wang H, Yao J, and Xie K (2007) Therapeutic inhibition of Sp1 expression in growing tumors by mithramycin a correlates directly with potent antiangiogenic effects on human pancreatic cancer. *Cancer* **110**:2682-2690.

Zhang Z, Song T, Zhang T, Gao J, Wu G, An L, and Du G (2011) A novel BH3 mimetic S1 potently induces Bax/Bak-dependent apoptosis by targeting both Bcl-2 and Mcl-1. *Int J Cancer* **128**:1724-1735.

MOL #81364

Zhou P, Levy NB, Xie H, Qian L, Lee CY, Gascoyne RD, and Craig RW (2001) MCL1 transgenic mice exhibit a high incidence of B-cell lymphoma manifested as a spectrum of histologic subtypes. *Blood* **97**:3902-3909.

Zhou P, Qian L, Bieszczad CK, Noelle R, Binder M, Levy NB, and Craig RW (1998) Mcl-1 in transgenic mice promotes survival in a spectrum of hematopoietic cell types and immortalization in the myeloid lineage. *Blood* **92**:3226-3239.

MOL #81364

### **Footnotes**

This work was supported by Basic Science Research Program through the National Research Foundation of Korea (NRF) funded by the Ministry of Education, Science and Technology [Grants 2012002481, 2012003731].

MOL #81364

## Figure Legends

### **Figure. 1 The over-expression of Mcl-1 is associated with anchorage-independent cell transformation in TPA or EGF-stimulated JB6 mouse skin epidermal cells.**

**A**, For the soft agar assay, JB6 cells were treated with various concentrations of TPA or EGF in 1ml of 0.3% basal medium Eagle's agar containing 10% FBS. Cells were incubated at 37°C in a 5% CO<sub>2</sub> incubator for 10 days, and then colonies were counted. The counted colonies were expressed as mean  $\pm$  SD. \*,  $P < 0.05$  compared with non-treated cells. **B**, JB6 cells were treated with activators of Mcl-1 promoter, TPA (20 ng/ml) or EGF (20 ng/ml) for different times (1, 2, 3, 6, 9 and 12 hr), and expression of Mcl-1 was analyzed by Western blots. **C**, JB6 cells were treated with DMSO or various concentrations of TPA or EGF for 3 hr and whole cell lysates were analyzed by Western blots. **D**, JB6 cells were transfected with siCon or siMcl-1 stimulated with TPA (20 ng/ml) or EGF (20 ng/ml), and a soft agar assay was carried out as described in the Materials and Methods. TPA or EGF-stimulated Mcl-1 expression in JB6 cells transfected with siCon or siMcl-1 was analyzed by Western blots.

### **Figure. 2 Mith modulates Mcl-1 expression and induce apoptosis in OSCC cells overexpressing Mcl-1.**

**A**, NOM tissues and OSCC tissues were immunostained using antibodies against Mcl-1. Levels of Mcl-1 were analyzed by immunostaining of fourteen NOM tissues samples and twenty-five OSCC tissues samples. Statistical differences ( $P < 0.05$ ) in Mcl-1 expression between NOM and OSCC tissues compared with NOM tissue samples is indicated (\*). Mcl-1 expression in various oral cancer cell lines was determined by Western blot analysis. **B**, Mcl-1 expression in HN22 and HSC4 cells treated with DMSO or various concentrations (15, 30, 60 nM) of Mith was determined by Western blots. Results are expressed as means  $\pm$  SD for

MOL #81364

triplicate experiments and significance ( $P<0.05$ ) compared with DMSO-treated cells is given (\*). **C**, Mcl-1 mRNA levels were confirmed by RT-PCR in both cells and normalized to  $\beta$ -Actin. Results are expressed as means  $\pm$  SD for triplicate experiments and significance ( $P<0.05$ ) compared to DMSO-treated results are indicated (\*). **D**, HN22 and HSC4 cells were treated with DMSO or 60 nM Mith for 6, 12, 24 and 48 hr, and whole cell lysates were analyzed by Western blots. **E**, For the soft agar assay, JB6 cells treated with TPA (20 ng/ml) or Mith incubated at 37°C in a 5% CO<sub>2</sub> incubator for 10 days, and colonies were counted as outlined in the Methods. HSC4 and HSC2 cells were treated with Mith incubated for 20 days, and then colonies were counted as described above. The significance ( $P<0.05$ ) of Mith-induced effects are indicated (\*) and results are expressed as means  $\pm$  SD for triplicate experiments.

**Figure. 3 Mith inhibits cell growth and induces apoptosis in OSCC cells.**

**A**, HN22 and HSC4 cells were treated with DMSO or various concentrations of Mith. Cell viability was determined using the MTS assay in both cells. The apoptotic effects of Mith in both cell lines were performed by Western blot analysis of whole cell lysates (**B**) and DAPI staining (**C**). **D**, HN22 and HSC4 cells were transfected with siCon or siMcl-1 for 72 hr, and then whole cell lysates were analyzed by Western blot analysis. **E**, The apoptotic effect of Mcl-1 siRNA was performed by DAPI staining. The DAPI-stained cell were quantified from triplicate experiments and significance ( $P<0.05$ ) by siMcl-1 compared with siCon are indicated (\*).

**Figure. 4 Down-regulation of Mcl-1 by Mith and RNAi regulates Bax induce apoptosis in OSCC cells.**

MOL #81364

**A**, Total Bax and activated Bax (6A7) were detected by Western blot analysis in HN22 and HSC4 cells. **B**, Mitochondrial fractions were prepared and analyzed by Western blots. Results are expressed as means  $\pm$  SD for 3 replicate experiments and significance ( $P < 0.05$ ) compared to DMSO is indicated. Cox4 was used to normalize the mitochondrial fraction. **C**, Bax oligomerization was detected in cell lysates after treatment with 0.2 mM BMH, and Western blot analysis as described in the Methods. **D** and **E**, Total Bax and activated Bax (6A7) were detected by Western blot analysis in HN22 and HSC4 cells transfected with siMcl-1. **F**, The cytosolic and mitochondrial fractions were from HN22 and HSC4 cells were analyzed by Western blots. Cox4 was used to normalize protein in mitochondrial fractions.

**Figure 5. Mith inhibits tumor growth and induces apoptosis in nude mouse xenograft models bearing HN22 cells.**

Athymic nude mice bearing HN22 cells as xenograft models were treated with DMSO or mithramycin A for 46 days, and tumor volume and tumor weights (**A**) and body weight (**B**) were determined. **C**, Tumor lysates from control and Mith-treated animals were analyzed for Mcl-1, Bax, Bax (6A7) and cleaved caspase-3 by Western blots. **D**, Apoptosis was detected in tumor tissues by TUNEL assay. **E**, Organ weight and Mcl-1 protein levels from five organs from control- and Mith-treated mice were determined by Western blots. **E**, Tissues from control- and Mith-treated mice were stained by hematoxylin and eosin as outlined in the Methods.

# Figure 1

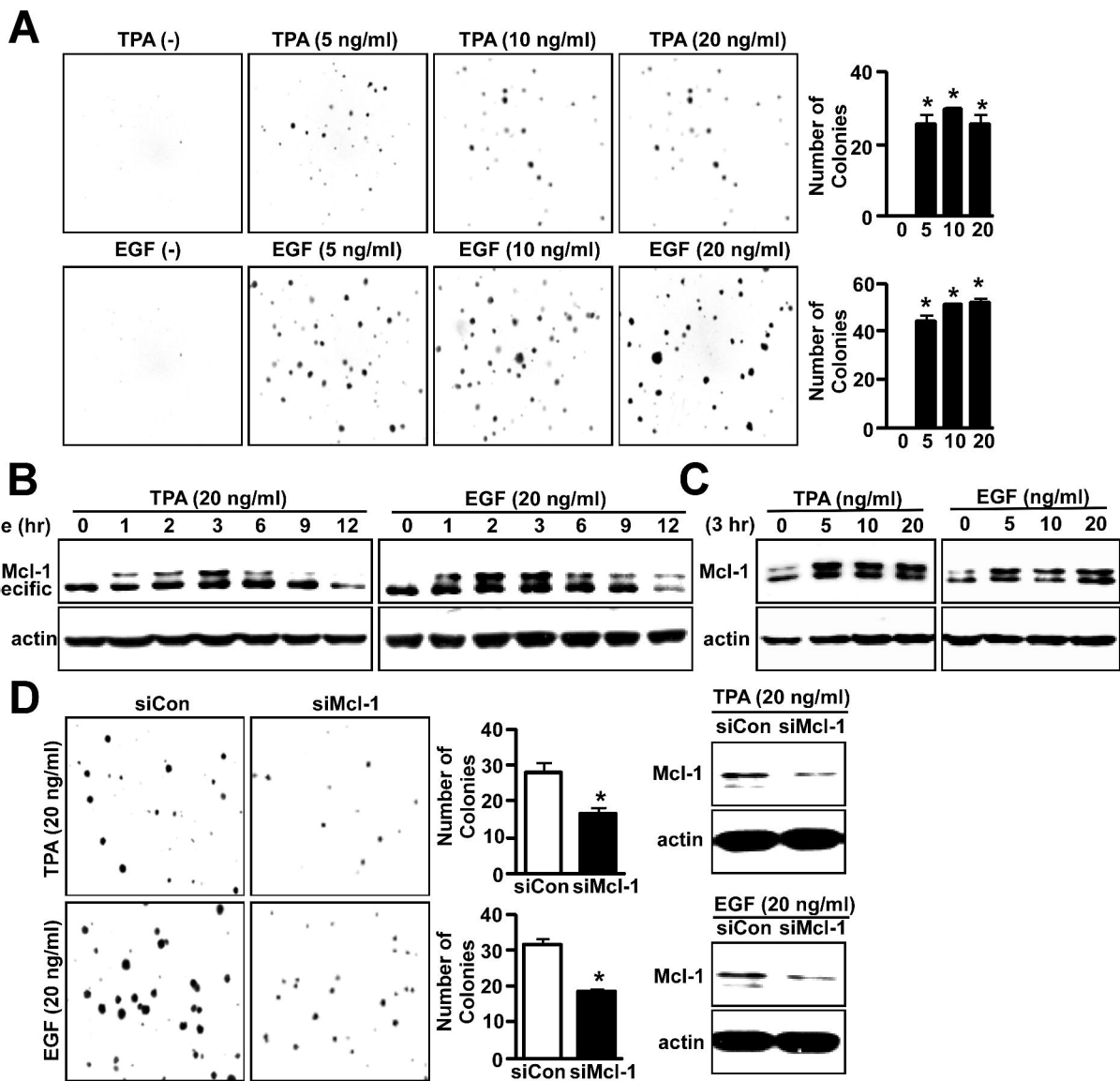
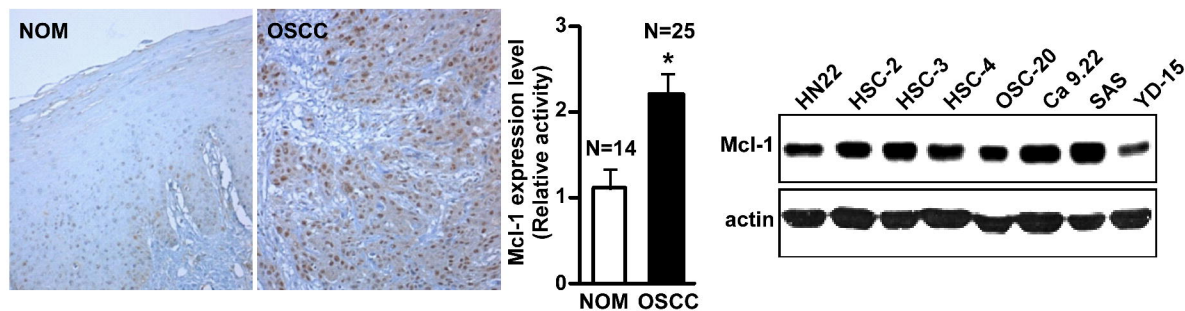
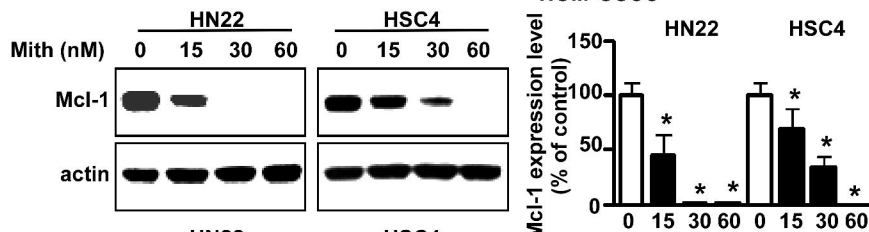


# Figure 2

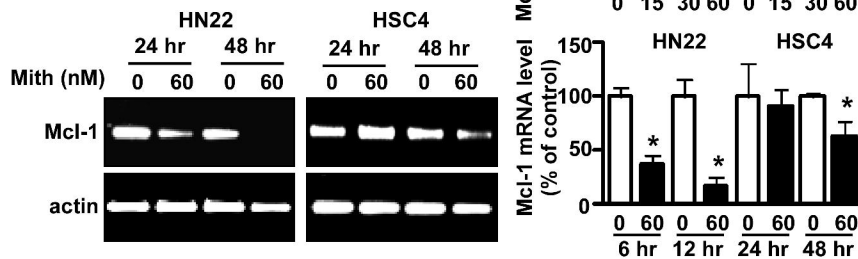
**A**



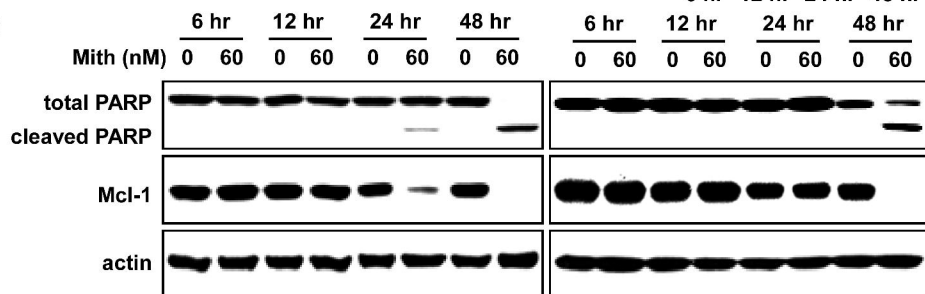
**B**



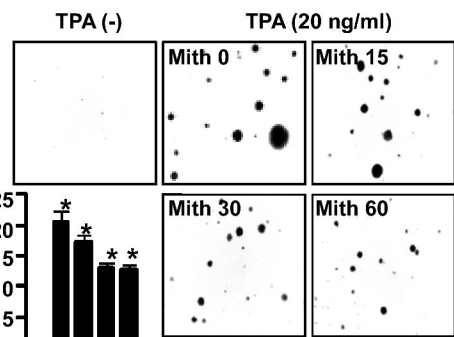
**C**



**D**



**E**



**F**

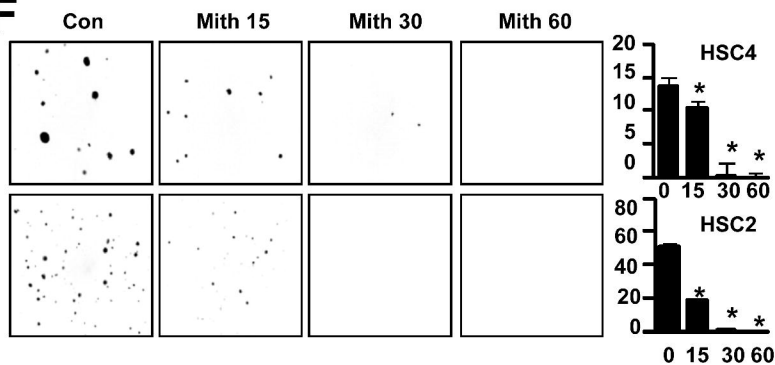




# Figure 3

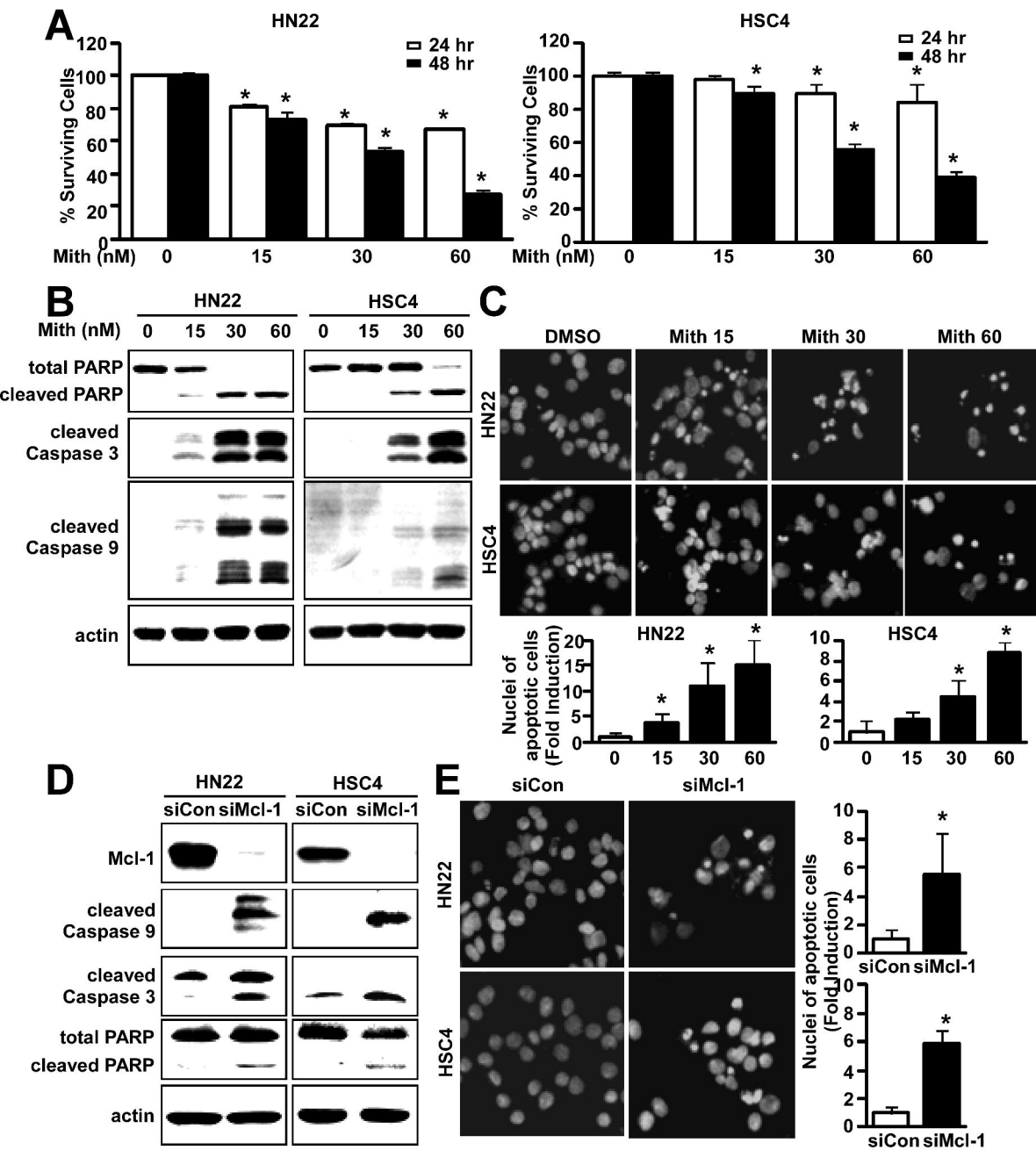
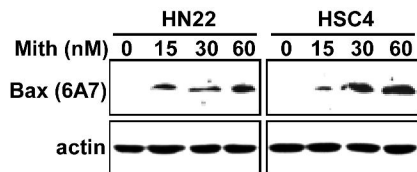
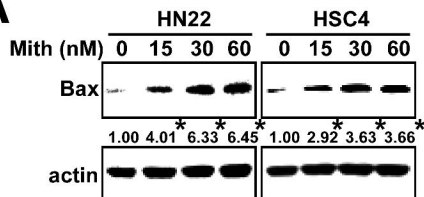
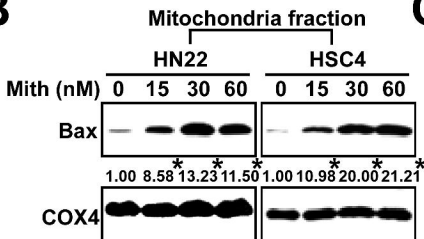


# Figure 4

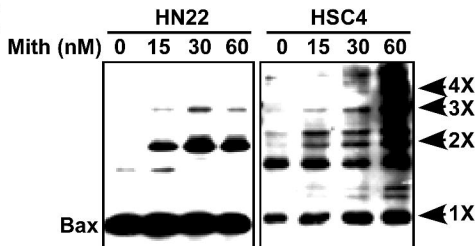
## A



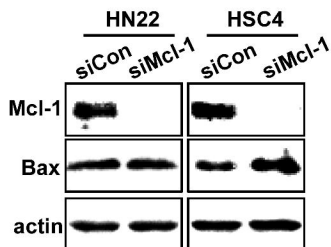
## B



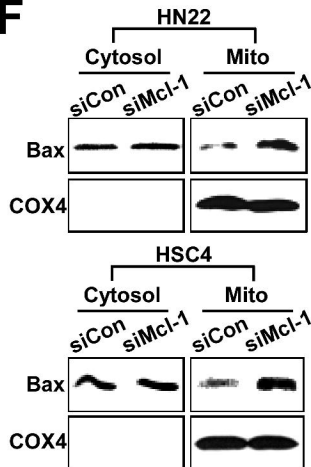
## C



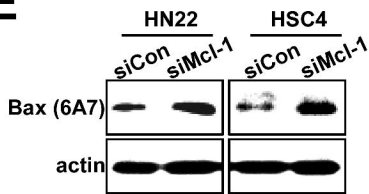
## D

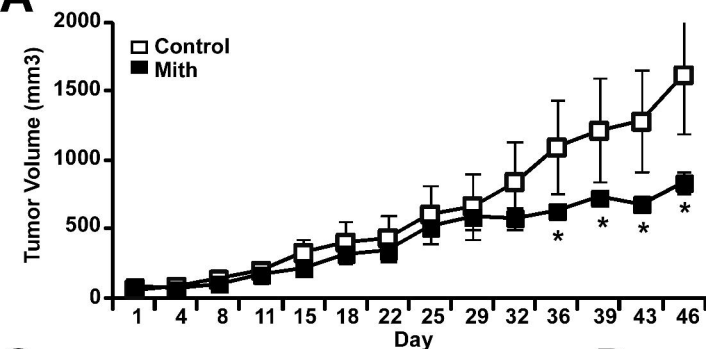
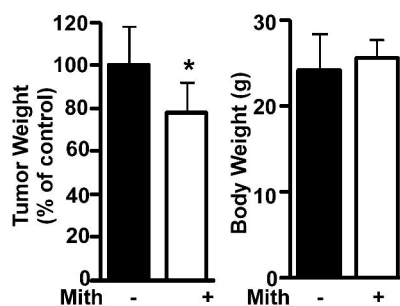
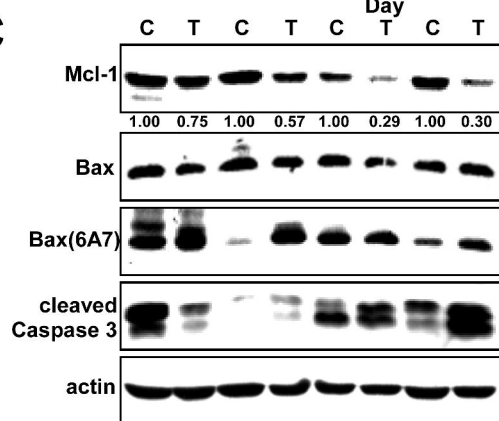
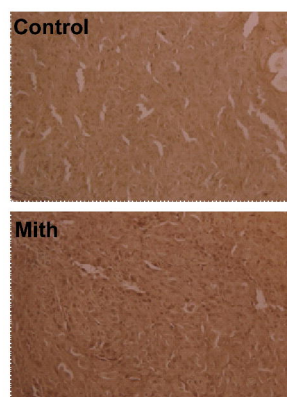
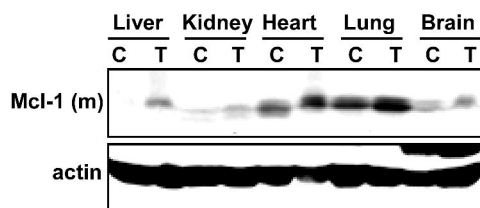
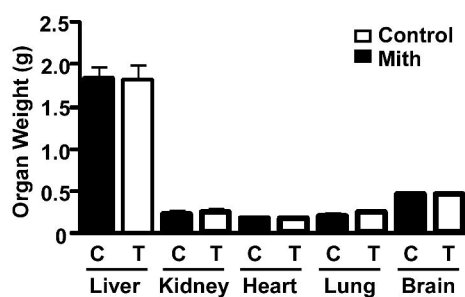


## F



## E



**Figure 5****A****B****C****D****E****F**